

# Synchrotron infrared near-field spectroscopy in photothermal mode

Chris S. Kelley,<sup>a</sup> Mark D. Frogley,<sup>a</sup> Ann Fitzpatrick,<sup>a</sup> Katia Wehbe,<sup>a</sup> Paul Donaldson<sup>b</sup> and Gianfelice Cinque<sup>a\*</sup>

<sup>a</sup>Diamond Light Source Limited, Harwell Science and Innovation Campus Didcot, Oxon OX11 0DE, UK.

E-mail: gianfelice.cinque@diamond.ac.uk

<sup>b</sup>Central Laser Facility, Research Complex at Harwell, Didcot, Oxon OX11 0FA, UK

Near-field infrared (IR) spectroscopy is revolutionising molecular imaging by allowing vibrational spectroscopic analysis at the sub-micrometre scale. We recently developed the world's first near-field IR photothermal microscope using synchrotron radiation (SR), which uniquely spans a spectral range from the near-IR to the far-IR/THz. Here we demonstrate the capability of the near-field method to probe polymer microspheres within a protein matrix, and we present the first IRSR photothermal near-field Fourier transform infrared (FT-IR) spectrum from within an individual biological cell, which establishes the feasibility of hyperspectral mapping at sub-micrometre resolution in a practical timescale. Photothermal near-field spectroscopy provides both depth sensitivity and IR molecular specificity, which is ideal for organic matter/biological samples. In addition, SR gives seamless and ultra-broadband spectral coverage superior to the bandwidth of commercially available lasers.

## Introduction

Until recently, the spatial resolution in infrared (IR) microspectroscopy was fundamentally limited to the scale of the wavelength due to optical diffraction and the limited numerical aperture of the microscope objectives. Even via synchrotron radiation (SR) IR beamlines, where a diffraction-limited microbeam is achievable,<sup>1</sup> or in a micro-attenuated total reflection (micro-ATR) geometry, where the high refractive index of, for example, a germanium crystal in contact with the sample enhances the magnification by up to four times, the spatial resolution in the information-rich fingerprint region of the mid-IR spectrum (500–1800 cm<sup>-1</sup>) is still limited to several micrometres. To overcome the spatial diffraction limit, near-field techniques are needed and pioneering measurements based on tip-scattering<sup>2</sup> and photothermal detection<sup>3</sup> have demonstrated that, by using an atomic force microscope (AFM) as a local probe, IR spectra can be obtained at a scale of just tens of nanometres. These two revolutionary nano-IR approaches have opened up a huge variety of

research avenues across many scientific disciplines.

The photothermal near-field method,<sup>3</sup> in which IR absorption is detected by the mechanical deflection of the AFM tip induced by the local thermal expansion of the sample, has several advantages: i) the IR spectrum produced is a true linear IR absorption; ii) it requires no numerical modelling of the signal to produce the spectrum; iii) it is not surface-limited in sensitivity since the whole volume of the sample is probed. Within their limited spectral range, latest generation IR laser sources can provide high quality near-field spectra in less than one minute and, with AFM tip resonance-enhanced techniques (RE-AFMIR), spectral signatures from nanoscale areas of samples as thin as a single molecular monolayer have been detected.<sup>4</sup>

We recently demonstrated that the brilliant, ultra-broadband, IRSR emitted by Diamond Light Source in the UK can be used to obtain near-field photothermal spectra by the RE-AFMIR method, at the sub-micrometre scale<sup>5</sup> within several minutes. In combination with the SR tip scattering approach first realised in the

THz,<sup>6</sup> then across the mid-IR region<sup>7,8</sup> and now under development at several SR facilities worldwide, these scientific tools find unique applications where the spectral bandwidth available from laser sources is a limitation.

In this article we present new experimental RE-AFMIR results from two sample types demonstrating the unique capabilities of the SR-based method. First, we look at a sample of polymer microspheres embedded within a protein layer, from which we are able to obtain broadband spectra and IR images of buried beads, and then we discuss the first data obtained by near-field photothermal IRSR from within an isolated human cell.

## Experimental

The SR resonance-enhanced AFM-IR system is schematically outlined in Figure 1. The broadband IR light generated from Diamond Light Source and collected by MIRIAM beamline B22<sup>1</sup> is collimated into a FT-IR interferometer (Bruker Vertex 80V). This is a Michelson set up where the IRSR beam is divided into two by the beamsplitter and reflected off two separate mirrors before being recom-

bined. The moving mirror (coloured blue in Figure 1) causes an intensity modulation of the broadband beam, where each optical wavelength is modulated at a unique temporal frequency. The FT-IR modulated SR beam is focused through a fast mechanical chopper, adding a further fast temporal on/off modulation to the beam intensity. The beam is then focused via a high numerical aperture Cassegrain IR objective (Agilent 15 $\times$ , NA 0.65) through the IR transparent substrate onto the sample.

At IR wavelengths where there is an absorption band of the material, the absorbed light power causes a very small temperature change (of order 10 mK) and consequent thermal expansion (sub-picometre) of the sample, which produces a deflection of the in-contact gold-coated silicon cantilever of the AFM (Nanonics MV1000). The AFM laser deflection signal from the position sensitive detector (PSD) is passed into a lock-in amplifier where only signals around the frequency of the chopper are amplified and therefore the weak, chopper modulated, deflection signal can be recovered within the environmental thermal background. This amplified signal still carries the FT-IR low frequency temporal modulation (interferogram), which is preserved in the thermal expansion of the sample, so the standard FT-IR software directly produces an IR spectrum comparable with conventional optical IR spectra.

Crucially, when the chopper modulation frequency is tuned to a mechanical contact resonance frequency of the AFM cantilever<sup>4</sup> the mechanical deflection is dramatically enhanced (of the order 100 $\times$  for a typical Si cantilever); this is key to obtain the IRSR-induced spectra on a practical timescale of a few minutes. The inverse of this chopper modulated frequency defines the measurement timescale, the thermal diffusion radius and therefore the spatial resolution.<sup>5</sup> In these experiments we used a harmonic of the fundamental cantilever resonance, between 60 kHz and 100 kHz, corresponding to about 1  $\mu$ m spatial resolution<sup>5</sup> for the materials studied here.

The dedicated set up is customised from a double infinity-corrected optical microscope (Nanonics) allowing both

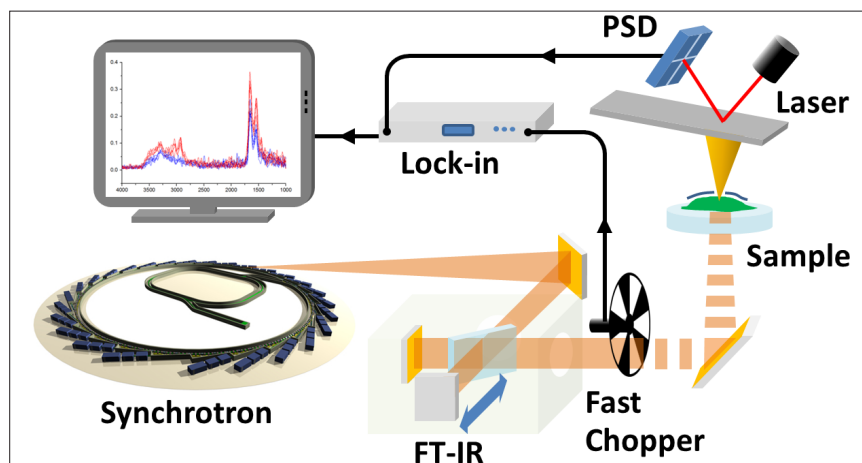


**Figure 1.** Schematic of the synchrotron RE-AFM-IR experiment.

top and bottom IR illumination and a visible camera view of the sample through identical Cassegrain objectives. The AFM is mounted on a large-range piezo-controlled x-y stage (PI), for precise positioning of the sample and AFM tip with respect to the IRSR microbeam focus. The sample is then scanned under the tip by the internal short-range piezo scanner of the AFM.

Polymer microbead samples were produced by mixing protein Bovine Serum Albumin (Sigma Aldrich) into a de-ionised water suspension of 1.04  $\mu$ m polystyrene (PS) beads (Bangs Laboratories, Inc.), then drop casting onto a CaF<sub>2</sub> substrate and dried in air. The preparation was tailored to produce samples in which the BSA covered the microbeads in most areas. The cell samples were formalin fixed *H. pylori* infected human cells (Bio-Quick Corp.) on a ZnS substrate.

## Results/discussion

Figure 2a shows an AFM topography image of the polystyrene (PS) beads/BSA sample recorded with an AFM tip of <100 nm (including gold coating). The height at some bead positions is less than 1  $\mu$ m above the surrounding BSA indicating that the beads are at least partially buried, however, from this topographical data we cannot determine if there is BSA on top of the bead or not. SR RE-AFMIR spectra recorded in positions on and off the beads (positions A and B in Figure 2a) are shown in Figure 2b, with the chopper frequency opti-

mally tuned to match the contact resonance in the two spatial positions. The spectrum obtained on pure BSA shows the expected IR bands for a protein, which are strong Amide I and II (1500–1700  $\text{cm}^{-1}$ ), Amide A (3300  $\text{cm}^{-1}$ ), and relatively weak C–H and O–H stretch bands (2750–3600  $\text{cm}^{-1}$ ). At the position of the PS bead, the strong C–H stretch bands of PS are observed along with a weaker shoulder due to the C–H bend (1425–1475  $\text{cm}^{-1}$ ) also characteristic of PS. The equivalent far-field IR absorbance spectra for individual BSA and PS samples<sup>9</sup> are shown in Figure 2c, confirming the expected spectral bands from each material.

Strikingly, in Figure 2b, the BSA is clearly contributing to the spectrum at the bead location (A) and the Amide I and II bands are even stronger than at the “background” position (B). This suggests that there is BSA covering the bead. It is worth noting that in this case a scattering near-field IR measurement would only be capable of detecting the BSA, and this depth sensitivity demonstrates one of the powerful advantages of the RE-AFMIR approach. Figure 2d shows the spectrally integrated RE-AFMIR signal recorded whilst scanning the topographic image in 20 minutes for the 10  $\times$  10  $\mu$ m scan. In this case the chopper frequency is tuned to the nominal contact resonance at the summit of the topography. This leads to some distortion of the RE-AFMIR image as the actual contact resonance varies with the sample to tip interaction changes.

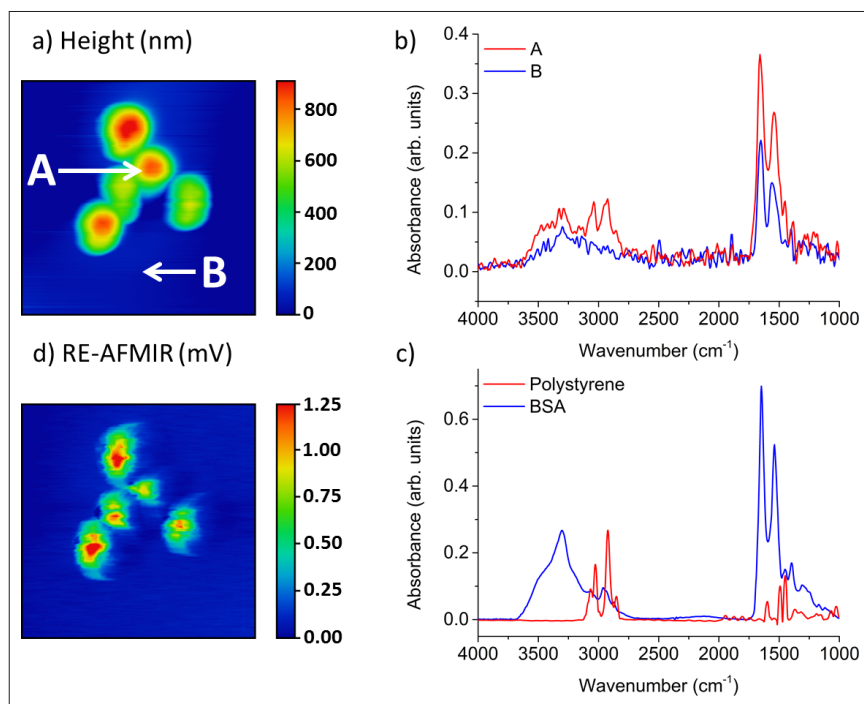


**Figure 2.** a) AFM topography image of PS beads embedded in BSA. b) SR RE-AFM-IR spectra recorded at A and B. c) Far-field (bulk) spectra of pure BSA and pure PS. d) SR RE-AFM-IR integrated signal map of the same area as a).

The ability of RE-AFMIR to resolve the chemical information from sub-surface beads was confirmed by imaging a larger sample area, this time using a quantum cascade laser source (QCL, Daylight Solutions) tuned to the aromatic C=C stretch band of PS at  $1601\text{ cm}^{-1}$  (Figure 3). The QCL was also mechanically chopped (50% duty cycle as with the SR) at a fixed frequency of the nominal contact resonance of the cantilever. The topography (Figure 3a) shows some broad undulating features, whilst the near-field IR signal (Figure 3b) in the same areas is essentially flat with well-

defined individual beads now clearly resolved. In particular, the raised region A in the topography image is completely absent in the IR map and several buried beads-barely observable in topography (B, C) appear as strong, well spatially resolved features in the  $1601\text{ cm}^{-1}$  absorbance map.

Large area RE-AFMIR imaging is also possible in reasonable times (tens of minutes) using the SR beam (Figure 2d) at present via the full spectrally integrated signal.

For the first time, we have been able to measure the SR near-field photother-

mal spectrum from a single human cell across the whole mid-IR region. This is expected to be a key area of application for the method, since the cellular organelles and structures are below the cell membrane. Figure 4 shows the AFM topography (a) and integrated SR RE-AFMIR signal map (b) of a single, fixed, bacterial infected human cell on a ZnS substrate. The typical cell IR spectrum, obtained in eight minutes, is clearly detectable above the background level of the substrate (shown for comparison) and with the expected features of biological matter<sup>10</sup> including Amide I and II dominated ( $1500\text{--}1700\text{ cm}^{-1}$ ) by proteins, Amide A and B ( $3100\text{ cm}^{-1}$  and  $3300\text{ cm}^{-1}$ ) and C-H stretch ( $2800\text{--}3150\text{ cm}^{-1}$ ) normally assigned to lipids, as well as the broad O-H band (*ca*  $3000\text{--}3700\text{ cm}^{-1}$ ). In addition, several bands in the fingerprint region corresponding to phosphates (DNA/RNA) and other groups are clearly evident; specifically, the symmetric and antisymmetric  $\text{PO}_2$ -stretches ( $1080\text{ cm}^{-1}$  and  $1243\text{ cm}^{-1}$ , respectively)<sup>11</sup> and the  $\text{CH}_3$  bend from proteins ( $1399\text{ cm}^{-1}$ ). Some of the apparent noise in the  $1250\text{--}1600\text{ cm}^{-1}$  region is likely due to residual atmospheric water vapour, which has not been corrected for. It is worth noting that no normalisation to the IRSR beam intensity spectrum has been performed, although this could be done for absolute quantification of the results. The FT-IR spectrum in Figure 4 demonstrates the feasibility of broadband SR RE-AFMIR mapping of a complete cell. In the current setup, at the spectral quality of Figure 4, a complete hyperspectral cell image over *ca*  $15 \times 15\text{ }\mu\text{m}$  square area will take approximately one day at  $1\text{ }\mu\text{m}$  spatial resolution. As the method is still in its infancy there is room for significant improvement in data quality as well as acquisition time as the technique is developed.

## Conclusions

We have measured the world's first broadband synchrotron-based near-field photothermal infrared spectrum from a  $1\text{-}\mu\text{m}$  region of an isolated biological cell in eight minutes, showing it is feasible to measure a complete hyperspectral map of a cell at this reso-

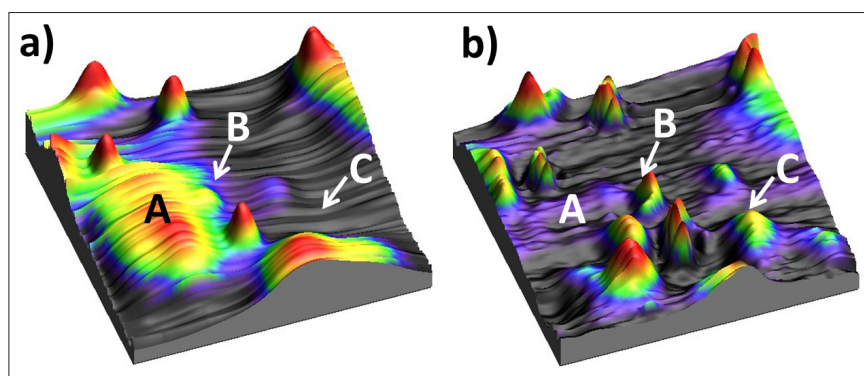


**Figure 3.** a) AFM topography of the PS bead/BSA sample. b) Single frequency RE-AFMIR image at the  $1601\text{ cm}^{-1}$  band of PS obtained with a QCL IR source.

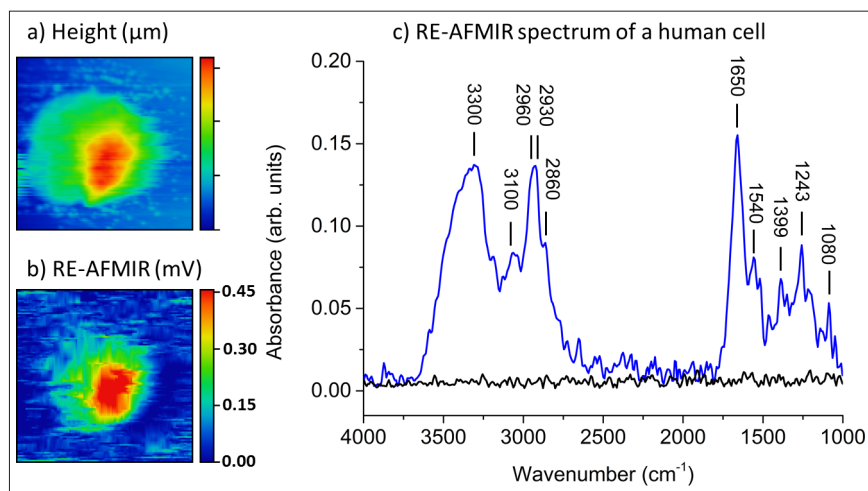


**Figure 4.** a) AFM topography of a single bacterial infected human cell. b) Integrated signal SR RE-AFMIR map acquired with the topography. c) SR RE-AFMIR spectrum from the cell in the region of peak integrated signal (blue), compared with background spectrum from the ZnS substrate (black).

lution within a day. Using polymer microbeads embedded in BSA, we have demonstrated the ability to spectrally resolve sub-surface features. This depth sensitivity and the direct, model-free FT-IR spectroscopy are clear advantages of the photothermal approach over the scattering based near-field method for many applications, whilst the use of synchrotron radiation gives access to a seamless ultra-broadband spectral range (Vis–THz) currently unmatched with laser sources. In the future we expect improvements in the technology to allow faster data acquisition rates and, using higher-resonance frequency cantilevers, spatial resolution approaching 100 nm.


## References

1. G. Cinque, M. Frogley, K. Wehbe, J. Filik and J. Pijanka, "Multimode InfraRed Imaging and Microspectroscopy (MIRIAM) beamline at Diamond," *Synchrotron Radiat. News* **24**, 24 (2011). doi: <https://doi.org/10.1080/08940886.2011.618093>
2. B. Knoll and F. Keilmann, "Near-field probing of vibrational absorption for chemical microscopy", *Nature* **399**, 134 (1999). doi: <https://doi.org/10.1038/20154>
3. A. Dazzi, R. Prazeres, F. Glotin and J.M. Ortega, "Local infrared microspectroscopy with an atomic force microscope tip used as a thermal sensor", *Opt. Lett.* **30**, 2388 (2005). doi: <https://doi.org/10.1364/OL.30.002388>
4. F. Lu and M.A. Belkin, "Infrared absorption nano-spectroscopy using sample photo-expansion induced by tunable quantum cascade lasers", *Opt. Express* **19**, 19942

5. P.M. Donaldson, C.S. Kelley, M.D. Frogley, J. Filik, K. Wehbe and G. Cinque, "Broadband


- near-field infrared spectromicroscopy using photothermal probes and synchrotron radiation", *Opt. Express* **24**, 1852 (2016). doi: <https://doi.org/10.1364/OE.24.001852>
6. U. Schade, K. Hollmack, P. Kuske, G. Wüstefeld and H.W. Hübers, "THz near-field imaging employing synchrotron radiation", *Appl. Phys. Lett.* **84**, 1422 (2004). doi: <https://doi.org/10.1063/1.1650034>
7. P. Hermann, A. Hoehl, P. Patoka, F. Huth, E. Rühl and G. Ulm, "Near-field imaging and nano-Fourier-transform infrared spectroscopy using broadband synchrotron radiation", *Opt. Express* **21**, 2913 (2013). doi: <https://doi.org/10.1364/OE.21.002913>
8. H.A. Bechtel, E.A. Muller, R.L. Olmon, M.C. Martin and M.B. Raschke, "Ultrabroadband infrared nanospectroscopic imaging", *Proc. Nat. Acad. Sci.* **111**, 7191 (2014). doi: <https://doi.org/10.1073/pnas.1400502111>
9. Data reproduced from Thermo-Fisher Scientific Spectral Libraries.
10. G. Bellisola and C. Sorio, "Infrared spectroscopy and microscopy in cancer research and diagnosis", *Am. J. Cancer Res.* **2**, 1 (2012).
11. P.T.T. Wong, E.D. Papavassiliou and B. Rigas, "Phosphodiester stretching bands in the infrared spectra of human tissues and cultured cells", *Appl. Spectrosc.* **45**, 1563 (1991). doi: <https://doi.org/10.1366/0003702914335580>

**EXPERTS in**  
**FLUORESCENCE SPECTROSCOPY**



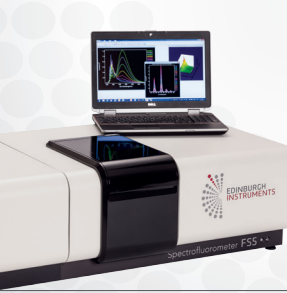
**EDINBURGH  
INSTRUMENTS**

**FLS980 Complete Luminescence Laboratory**



- > Research-grade fluorescence spectrometer
- > Single photon counting, Fluorescence lifetimes (TCSPC) and Phosphorescence lifetimes (MCS)
- > >25,000:1 Water Raman SNR
- > Multiple sources and detectors
- > Upgrades include - NIR coverage, microscopes, plate reader module, polarisation, integrating sphere and more

**FS5 Photon Counting Spectrofluorometer**



- > Fluorescence and phosphorescence measurements capability, including lifetimes, up to 1650 nm
- > >6,000:1 Water Raman SNR, the most sensitive bench-top fluorometer available
- > Transmission detector for UV-VIS absorption spectroscopy
- > UV-VIS-NIR range

sales@edinst.com | www.edinst.com